Metallic-like thallium overlayer on a Si(111) surface

Pavel Kocán,[*] Pavel Sobotík, and Ivan Ošt'ádal

Charles University in Prague, Faculty of Mathematics and Physics, Department of Surface and Plasma Science, V Holešovičkách 2,
180 00 Praha 8, Czech Republic

A (1×1) ordered monolayer of thallium atoms on a Si(111) surface has promising potential as a material generating spin-polarized electrons [Sakamoto *et al.*, Phys. Rev. Lett. **102**, 096805 (2009)]. In an ideal form the surface is nonmetallic [Lee *et al.*, Phys. Rev. B **66**, 233312 (2002)]. Our scanning-tunneling microscopy and spectroscopy study of the (1×1)-Tl surface shows clearly its metallic-like character. On the surface, intrinsic regularly shaped defects with increased density of states near the Fermi level are observed. The relationship between the presence of the defects, which we interpret as Tl multivacancies induced by Si adatoms, and metallicity of the layer is briefly discussed.

A great challenge nowadays is to provide background for utilizing the spin of electrons in new devices. Recently, Rashba spin splitting was reported for the Pb/Ge(111) system[1] with the split band crossing the Fermi level. In applications, compatibility of spintronic elements with silicon technology would be a significant advantage. On a silicon substrate, Rashba spin splitting was observed in the case of a Tl/Si(111)-(1×1) surface.[2] However, this surface is not metallic-like, and transfer of spin-polarized electrons is difficult. Thus, motivation is high for studying possibilities of doping the surface on an atomic level.

With miniaturization of semiconductor electronic elements trending downward to sizes of hundreds of interatomic lengths, each individual dopant becomes crucial to a component's functioning.[3] The possibility of mapping dopants on an atomic scale is therefore of great value.[4]

Deposition of one monolayer (ML, 7.83×10^{14} atoms cm^{-2}) of Tl on a Si(111) surface and annealing to 300–350 °C results in formation of a (1×1) Tl reconstruction. Its structure has been studied by various techniques: low-energy electron diffraction,[5] synchrotron x-ray scattering,[6] and *ab initio* calculations.[7] It is agreed that Tl atoms occupy T_4 sites of a bulk-terminated Si(111) surface. The structure is stabilized by a charge transfer from the Tl adlayer to the topmost silicon atoms, Tl $6p$ electrons are partially donated to dangling bonds of the Si atoms, which become fully saturated.[7] According to angle-resolved photo-emission spectroscopy and calculations using density-functional theory (DFT), the Tl/Si(111)-(1×1) surface is semiconducting with a band gap of 0.34 eV.[7] Scanning tunneling spectroscopy (STS) on the Tl/Si(111)-(1×1) surface reported by Vitali *et al.*[8] supported the semiconducting character with a surface state band gap of ~0.5 eV.

If surface concentration of Tl atoms is decreased by desorption from the (1×1) layer, a Tl/Si(111)-($\sqrt{3} \times \sqrt{3}$) reconstruction forms.[7] A band gap of 0.3 eV was calculated for this structure,[9] in agreement with results of a photoemission study.[10]

In both (1×1) and ($\sqrt{3} \times \sqrt{3}$) phases, Tl $6s^2$ electrons are chemically inactive[11] due to a so called inert pair effect, making the Tl behavior different from the other—strictly trivalent—group III metals.

In the case of the Tl/Ge(111)-(1×1) surface, which is iso-electronic to Tl/Si(111)-(1×1), a band crossing the Fermi level was observed by angle-resolved photo-emission spectroscopy (ARPES).[12] Because *ab initio* calculations did not confirm the metallic character, the authors proposed that the band crossing the Fermi level is caused by intrinsic Tl vacancies acting as acceptor dopants.[12]

In this Brief Report we present observations of the metallic-like Tl/Si(111)-(1×1) surface, as revealed by scanning-tunneling microscopy (STM) and spectroscopy. On the surface, we recognize ring-shaped objects, the structure of which is discussed. Following the proposals for the Tl/Ge(111)-(1×1) surface we discuss possible doping behavior of these objects.

For experiments, Si(111) samples (Sb doped, with a resistivity of 0.005–0.01 Ω cm) were cleaned by flashing to 1200 °C. Thallium (purity 99.999%) was evaporated onto the silicon surface at room temperature, with the amount controlled by a quartz thickness monitor. The Tl/Si(111)-(1×1) surface was prepared by heating the sample with one predeposited monolayer of Tl to 300 °C for 2 min. The STM and STS measurements were performed by using a non-commercial scanning tunneling microscope in an ultrahigh-vacuum chamber with base pressure $< 3 \times 10^{-9}$ Pa. The pressure during the Tl deposition was in the 10^{-8} Pa order. STS curves were obtained using a lock-in technique (~10 s per spectrum), and the reported data were averaged over several equivalent spectra normalized by I/V. Noise in the data near the Fermi level was suppressed by a procedure noted in Ref. 13. In addition, fast $I(V)$ curves (~50 ms per curve) were measured separately. All presented data were acquired at room temperature.

First we focus on STM imaging of the Tl/Si(111)-(1×1) surface. An STM image of the Si(111) surface after deposition of 1 ML of Tl and subsequent annealing to ~300 °C is shown in Fig. 1(a). On the terraces, many craterlike objects are observed. Most of the objects are regularly ring shaped, and others are formed by several ring-shaped objects merging together. Typically, concentration of the objects (hereafter called defects) is in the range of 0.5–1 × 10^{13} cm^{-2}.

To study the influence of preparation conditions on formation of the defects, different preparation procedures were tested as well: deposition of 1 ML of Tl on a surface held at 300 °C,
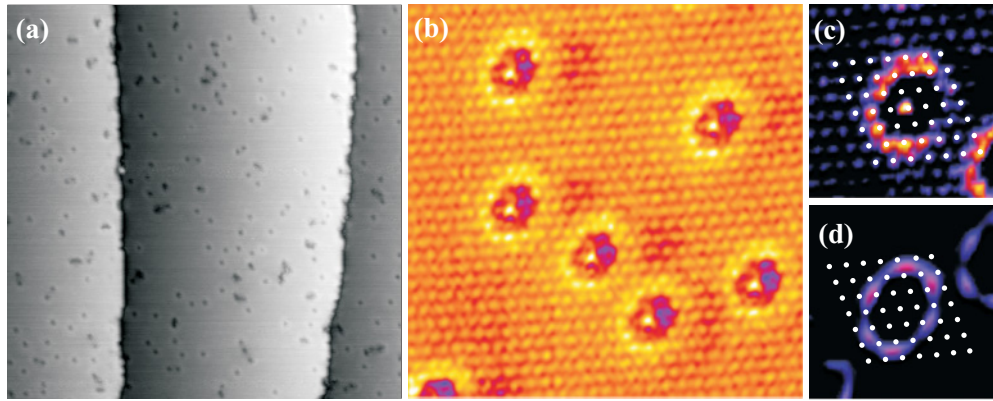
FIG. 1. (Color online) (a) Empty-state STM image of the (1×1) surface with defects (area 50×50 nm^2, sample voltage $U_s = 0.2$ V, and $I = 0.7$ nA). (b) Detail of the (1×1) structure with ring-shaped defects (area 7×7 nm^2, $U_s = 9$ mV, and $I = 2.2$ nA). (c) Detail of the defect, zoomed out from (b) (area 2.7×2.7 nm^2). (d) The same scale as in (c) but recorded at $U_s = 0.44$ V. The color contrast is adjusted to highlight a ring surrounding the defect. Dots in (c) and (d) mark equivalent positions in the 1×1 grid.

varying the temperature to a lower limit of (1×1) formation, and deposition of slightly more or less than 1 ML. All the procedures resulted in the presence of the defects once the (1×1) structure was formed, and the concentration of the defects was not observed to depend strongly on the preparation procedure.

A detail $(7 \times 7$ nm$^2)$ of the surface obtained at a significantly low sample-tip bias of 8 mV is shown in Fig. 1(b). The (1×1) reconstruction is clearly visible together with the ring-shaped defects. A magnified detail $(2.7 \times 2.7$ nm$^2)$ of a defect taken from Fig. 1(b) is shown in Fig. 1(c). On the image, the defect is dominated by 12 spots of the 1×1 pattern forming a ring brighter than the 1×1 protrusions far from the defects. We note that the bright ring is not a result of STM feedback, since the same images are observed in both scanning directions (not shown). The most probable explanation of the bright ring lies in the surface states originating from the presence of the defects. In the middle of the ring, another bright protrusion is observed. This central protrusion is visible only at low sample voltage, disappears at $\sim \pm 200$ mV, and is not reproduced at all tip apex conditions. The area between the central protrusion and the surrounding ring appears darker than the 1×1 surface far from the defects. A detail of the defect obtained with the same tip as in Fig. 1(c) but at higher sample voltage (0.44 V) is shown in Fig. 1(d). The size and orientation of the defect is the same as in Fig. 1(c). At this voltage, the 1×1 corrugation and the central protrusion disappear, and the apparent shape of the ring is different, now being composed of six prolonged protrusions. When imaging occupied states close to the Fermi level (sample voltage ~ -40 mV), the STM pattern of the defect (not shown) is similar to that at low positive voltages: a highlighted ring surrounding a crater. The 1×1 pattern is less corrugated at the negative biases. At higher negative sample voltages $(\sim -0.2$ V), the bright ring disappears and the defect looks like a hole on the surface.

Over the STM details of defects in Figs. 1(c) and 1(d), the 1×1 grid of white dots is superimposed as a guide. For discussion of a structural model, we suppose that these dots and the corresponding protrusions in Fig. 1(c) are located in the T_4 sites occupied by the Tl atoms.[14]

STM imaging at a bias of a few millivolts is the first indication that the surface is metallic, in contradiction with

the reported ARPES and STM results and with *ab initio* calculations.[7,8] In order to show the surface metallicity, we measured dI/dV tunneling spectra near the Fermi level. STS taken at a (1×1) area is shown in Fig. 2(a) by the solid line. For comparison, a spectrum taken at a Tl-$(\sqrt{3} \times \sqrt{3})$ area by the same tip and under the same conditions is shown by the broken line in Fig. 2(a). The $(\sqrt{3} \times \sqrt{3})$ area was locally formed on the otherwise (1×1) surface with defects, as shown in Fig. 2(b). The STS spectra from Tl-$(\sqrt{3} \times \sqrt{3})$ exhibit a band gap of ~ 0.4 eV, which is in a good agreement with a value of 0.3 eV measured[10] and calculated[9] previously. In contrast, the surface local density of states of the (1×1) area is nonzero at the Fermi level. The increase of density of states at negative and positive sample voltages is possibly related to the surface states S_1 and S_2 from Ref. 7, respectively.[15] In addition to the spectra measured by the lock-in technique that are in principle sensitive to a phase shift between the reference and measured signals, we recorded a fast (50 ms per curve) I-V
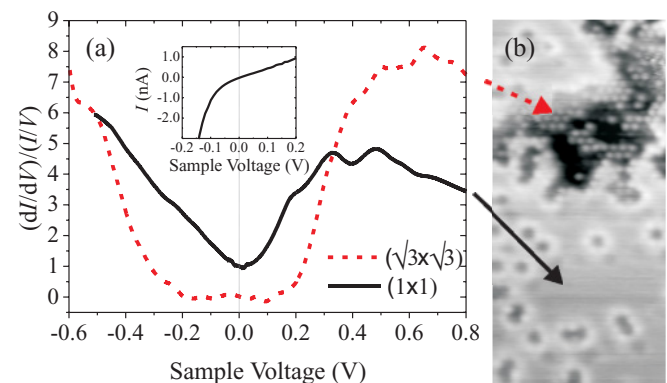

FIG. 2. (Color online) (a) Normalized tunneling spectra $(dI/dV)/(I/V)$ on the (1×1) (solid line) and $(\sqrt{3} \times \sqrt{3})$ (broken line) surfaces, showing nonzero density of states of the (1×1) surface at the Fermi level. Inset: fast I-V characteristic measured separately on the (1×1) surface. (b) STM image of the surface with coexisting (1×1) (solid arrow) and $(\sqrt{3} \times \sqrt{3})$ (broken arrow) areas, used for measuring $(dI/dV)/(I/V)$ data in (a). Image size 9×18 nm^2, $U_s = 1.0$ V.
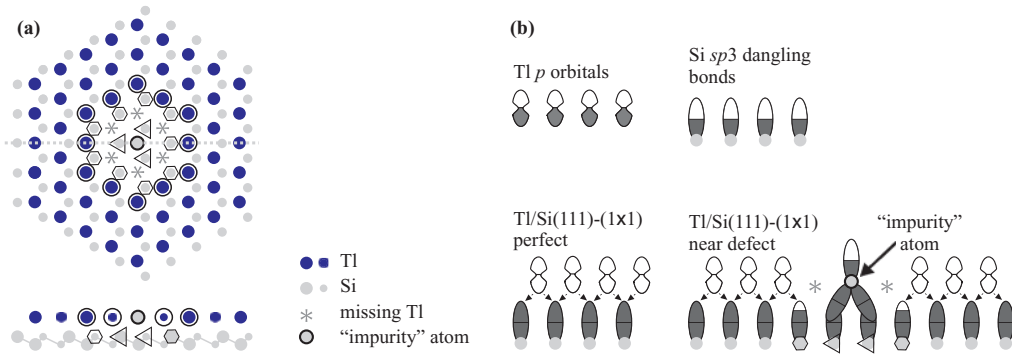
FIG. 3. (Color online) (a) Top and side schematic views of a possible model of Tl multivacancy observed on the (1×1) surface. Dark and light circles denote Tl and Si atoms, respectively. Selected positions are marked. Triangles: Si atoms to which central "impurity" atom is bonded. Asterisks: Tl vacancies. Hexagons: Si atoms with less than three Tl neighbors. Large circles: Tl atoms forming a ring shape on the STM images. (b) A simple electron bond filling scheme of surface orbitals (depicted by ovals) near the vacancy. Occupation of orbitals is represented by gray shading.

characteristic on the (1×1) surface. The result is shown in the inset of Fig. 2(a). Obviously, slope of the $I(V)$ curve at zero bias (Fermi level) is nonzero, showing the metallicity of the surface.

We continue by discussing the possible origin of the defects. First we exclude simple Tl vacancies because the defects were observed even at deposited amounts exceeding one monolayer. Another possible origin of the defect could be a relic of the 7×7 reconstruction containing a structural fault.[16] However, concentration of such defects would depend on annealing temperature, in contrast to our experimental findings. Thus, impurity atoms are likely to be responsible for the defects. The first possible impurity would be Sb, because we used highly Sb-doped samples for experiments. However, volume dopant concentration in the samples was $\sim0.01\%$, which is not sufficient for the observed surface concentration ($\sim1\%$) of the defects. A significant segregation of Sb at surface could be excluded, because Sb desorbs from the Si(111) surface at $\sim750\,^{\circ}\mathrm{C}$[17] and the sample was annealed to $1200\,^{\circ}\mathrm{C}$ prior to every experiment. The most probable "impurities" in the Tl layer remain Si atoms residual of the Si-rich (7×7) reconstruction. We note that Si adatoms tend to substitute for Tl atoms during Tl desorption, which results in formation of a mosaic $(\sqrt{3}\times\sqrt{3})$ surface.[18] Moreover, isolated Si adatoms from the $(\sqrt{3}\times\sqrt{3})$ mosaic[18] resemble the defects shown in Fig. 1(b). Even though we cannot completely exclude other impurities causing defects (e.g., from residual atmosphere), Si adatoms seem to be the most probable.

A possible structural model of the ring-shaped defects is schematically depicted in Fig. 3(a). In the figure, the light and dark circles denote Si and Tl atoms, respectively. Assume an "impurity" Si adatom is adsorbed instead of Tl in the central T_4 position, marked by the light-filled dark-outlined circle in Fig. 3(a). The adatom saturates dangling bonds of three nearest surface Si atoms (marked by triangles). As the dangling bonds are saturated, six T_4 positions neighboring the saturated Si atoms are not occupied by Tl atoms (the vacancies are marked by asterisks). Nine Si atoms marked by hexagons neighbor only two or one Tl atoms, while in the perfect (1×1) structure there are three neighbors. We note that a similar model with the central impurity adatom adsorbed in the H_3 position can

be constructed as well. In that case, the protrusions forming the ring [with the same size as the ring in Fig. 3(a)] and the 1×1 protrusions would appear in the H_3 positions. To confirm one of the two models, *ab initio* calculations would be needed.

Next we discuss a possible influence of the multivacancy defect on the surface properties. A simplified charge-transfer consideration of the atomic arrangement is schematically depicted in Fig. 3(b). Before the interaction, Tl p orbitals and dangling bonds of an ideal Si(111)-(1×1) termination are half filled [top of Fig. 3(b)]. During formation of the perfect Tl/Si(111)-(1×1) reconstruction, every Si dangling bond is saturated by a charge transferred from the Tl orbitals [effectively one third of electrons from each of the three neighboring Tl atoms; bottom left of Fig. 3(b)].[7] According to DFT calculations of an isoelectronic Tl/Ge(111)-(1×1) surface,[12] the Tl $6p$ state is not emptied completely; the highest occupied surface state has partial $p_x + p_y$ character and is separated by a band gap from the lowest unoccupied band. If a Tl vacancy is created, the neighboring Si atoms (marked by hexagons in Fig. 3) lack the charge from the missing Tl atoms, as indicated in the right-hand-side bottom part of Fig. 3(b). This charge deficit can possibly be partially balanced by redistribution of charge from the next nearest neighboring Si dangling bonds, from the partially occupied Tl $6p_x + p_y$, orbitals, or by charge transfer from the "impurity" atom orbitals. Such charge transfer may be accompanied by relaxation of atomic positions and by relief of strain in the epitaxial layer. The structural relaxation and charge redistribution may result in significant modification of the density of states at the Fermi level.

In Ref. 12, a hole-doping behavior of Tl vacancies was proposed to explain photoemission results. In such cases, the position of the Fermi level would be shifted to the valence band. From our STS observation, we cannot confirm this simple picture, since the band gap is not shifted but is completely reduced. Our results suggest that the metallic-like character of the surface is a consequence of more complex surface structural relaxation and charge redistribution.

In conclusion, observation of the metallic character of the Tl/Si(111)-(1×1) surface is reported in contrast with the previous experimental and theoretical work. The regularly shaped vacancies observed on the surface are proposed to be

responsible for metallicity of the 2D adlayer. The Tl vacancies give arise to an increase of the density of states near the Fermi level as measured by STS. Consequently, the dopants can be mapped by STM at very low biases.

---

[*]pavel.kocan@mff.cuni.cz

[1]K. Yaji, Y. Ohtsubo, S. Hatta, H. Okuyama, K. Miyamoto, T. Okuda, A. Kimura, H. Namatame, M. Taniguchi, and T. Aruga, Nature Commun. **1**, 17 (2010).

[2]K. Sakamoto, T. Oda, A. Kimura, K. Miyamoto, M. Tsujikawa, A. Imai, N. Ueno, H. Namatame, M. Taniguchi, P. E. J. Eriksson, and R. I. G. Uhrberg, Phys. Rev. Lett. **102**, 096805 (2009).

[3]S. Roy and A. Asenov, Science **309**, 388 (2005).

[4]M. R. Castell, D. A. Muller, and P. M. Voyles, Nature Mater. **2**, 129 (2003).

[5]T. Noda, S. Mizuno, J. W. Chung, and H. Tochihara, Jpn. J. Appl. Phys. **42**, L319 (2003).

[6]N. D. Kim, C. G. Hwang, J. W. Chung, T. C. Kim, H. J. Kim, and D. Y. Noh, Phys. Rev. B **69**, 195311 (2004).

[7]S. S. Lee, H. J. Song, N. D. Kim, J. W. Chung, K. Kong, D. Ahn, H. Yi, B. D. Yu, and H. Tochihara, Phys. Rev. B **66**, 233312 (2002).

[8]L. Vitali, M. G. Ramsey, and F. P. Netzer, Surface Sci. **452**, L281 (2000).

[9]S. Özkaya, M. Çakmak, and B. Alkan, Surface Sci. **602**, 1376 (2008).

[10]K. Sakamoto, P. E. J. Eriksson, N. Ueno, and R. I. G. Uhrberg, Surface Sci. **601**, 5258 (2007).

[11]K. Sakamoto, P. E. J. Eriksson, S. Mizuno, N. Ueno, H. Tochihara, and R. I. G. Uhrberg, Phys. Rev. B **74**, 075335 (2006).

[12]S. Hatta, C. Kato, N. Tsuboi, S. Takahashi, H. Okuyama, T. Aruga, A. Harasawa, T. Okuda, and T. Kinoshita, Phys. Rev. B **76**, 075427 (2007).

[13]M. Prietsch, A. Samsavar, and R. Ludeke, Phys. Rev. B **43**, 11850 (1991).

[14]From our STM images we cannot strictly decide which site corresponds to the protrusions in Fig. 1(c). According to *ab initio* calculations, the lowest unoccupied orbitals should be Tl $6p_x + 6p_y$.[12] However, the exact location of the protrusions with respect to Tl atoms is not known.

[15]Note the unusual notation in Ref. 7: S_1 for the highest occupied state and S_2 for the lowest unoccupied state.

[16]A. Zotov, A. Saranin, V. Kotlyar, O. Utas, and Y. Wang, Surface Sci. **600**, 1936 (2006).

[17]H. Guesmi, L. Lapena, G. Tréglia, and P. Müller, Phys. Rev. B **77**, 085402 (2008).

[18]V. G. Kotlyar, A. A. Saranin, A. V. Zotov, and T. V. Kasyanova, Surface Sci. **543**, L663 (2003).